



HAL
open science

Efficiency of benthic diatom-associated bacteria in the removal of benzo(a)pyrene and fluoranthene

Oumayma Kahla, Sondes Melliti Ben Garali, Fatma Karray, Manel Ben Abdallah, Najwa Kallel, Najla Mhiri, Hatem Zaghden, Badreddine Barhoumi, Olivier Pringault, Marianne Quemeneur, et al.

► **To cite this version:**

Oumayma Kahla, Sondes Melliti Ben Garali, Fatma Karray, Manel Ben Abdallah, Najwa Kallel, et al.. Efficiency of benthic diatom-associated bacteria in the removal of benzo(a)pyrene and fluoranthene. Science of the Total Environment, 2021, 751, pp.141399. 10.1016/j.scitotenv.2020.141399 . hal-02925530

HAL Id: hal-02925530

<https://hal.science/hal-02925530>

Submitted on 29 Apr 2022

HAL is a multi-disciplinary open access archive for the deposit and dissemination of scientific research documents, whether they are published or not. The documents may come from teaching and research institutions in France or abroad, or from public or private research centers.

L'archive ouverte pluridisciplinaire **HAL**, est destinée au dépôt et à la diffusion de documents scientifiques de niveau recherche, publiés ou non, émanant des établissements d'enseignement et de recherche français ou étrangers, des laboratoires publics ou privés.

35 **Abstract**

36 A benthic diatom *Nitzschia sp.*, isolated from a PAH-contaminated sediment, was exposed in
37 axenic and non-axenic cultures to BaP and Flt over 7 days. The diversity of the associated bacteria,
38 attached (AB) and free-living bacteria (FB), was analyzed by the MiSeq-derived 16S rRNA. The
39 diatom was able to grow under BaP and Flt treatments and to accumulate both PAHs.
40 Biodegradation, which constituted the main process for PAH elimination, was enhanced in the
41 presence of bacteria. Diatom and bacteria showed different capacities in the degradation of PAHs.
42 The attached bacteria exhibited higher diversity and abundance relative to free-living bacteria,
43 while the FB fraction contained genera with the known ability of PAH degradation. Isolated strains
44 from the FB community, showed the capacity to grow in the presence of crude oil. These results
45 suggest that a “benthic *Nitzschia sp.*-associated hydrocarbon-degrading bacteria” consortium can
46 be applied in the bioremediation of PAH-contaminated sites.

47 **Key words**

48 Accumulation, biodegradation, Bizerte Lagoon, *Nitzschia sp.* phycosphere, hydrocarbon-
49 degrading bacteria

50

51

52 **1. Introduction**

53 Marine pollution through chemical contaminants has become a matter of great concern
54 because of its deleterious impacts on marine ecosystems. Polycyclic aromatic hydrocarbons
55 (PAHs) are among the most hazardous pollutants, with potential harmful effects on biota and
56 ecosystems (Hylland, 2006). They are hydrophobic and ubiquitous pollutants detected in all
57 ecosystems, from polar regions to the tropics (Wilcke, 2007; Duran and Cravo-Laureau, 2016).

58 Sixteen PAHs have been included in the US Environmental Protection Agency's list of priority
59 pollutants (US-EPA). Because of their strong toxicity, persistence, and accumulation in marine
60 animals and plants, a great deal of attention has been paid to the elimination and degradation of
61 PAHs (Duran and Cravo-Laureau, 2016; González-Gaya et al., 2019). Physicochemical and
62 thermal techniques are used in several processes of soil or sediment treatments, but biological
63 remediation has been recognized as the most efficient method for decontaminating environments
64 polluted by PAHs. Indeed, PAHs are biodegraded by a wide range of microorganisms (McKew et
65 al., 2007, Gutierrez, 2013, Thompson et al., 2017). Among them, bacteria are considered as the
66 dominant agents in hydrocarbon biodegradation, and several marine hydrocarbon-degrading
67 isolates have been described worldwide (Ben Said et al., 2008; Haritash and Kaushik, 2009;
68 Jiménez et al., 2011). Thus, "marine bacterial consortia" have been widely used in efforts to
69 depollute environments contaminated by PAH mixtures and oil, such as harbors and wastewater
70 effluents, or during oil spills (Arulazhagan and Vasudevan, 2009, Jiménez et al., 2011). Microalgae
71 can also play a significant role in the removal of PAHs. Warshasky et al. (1988) have shown that
72 the freshwater microalgae *Selenastrum capricornitum* was able to metabolize benzo(a)pyrene
73 (BaP) to cis-dihydrodiols through a system of enzyme dioxygenases such as that found in bacteria.
74 Two diatom species, *Nitzschia* sp. and *Skeletonema costatum*, can accumulate and degrade
75 phenanthrene (Phe) and fluoranthene (Flt) (Hong et al., 2008). Diatoms of the genus *Pseudo-*
76 *nitzschia* have recently been reported to accumulate and degrade a mixture of PAHs (Melliti Ben
77 Garali, 2016). Other studies have reported that Phe and pyrene (Pyr) could be converted by
78 photosynthetic microorganisms into soluble diols, phenols, lactones, naphthoic acid, and phthalic
79 acid, which may be excreted in the overlying water column (Seo et al., 2007).

80 Other works have demonstrated that a "microalgae-bacteria consortium" could be
81 successfully used in the treatment of aromatic pollutants ((Borde et al., 2003; Muñoz et al., 2003).
82 There is a synergetic relationship between algae and bacteria, in which algae provide oxygen

83 (through photosynthesis) required by aerobic bacteria in the aerobic biodegradation of PAHs. In
84 turn, bacteria produce carbon dioxide for photosynthetic metabolism. [Borde et al. \(2003\)](#) have
85 shown that the removal of Flt and Pyr was better (up to 85%) when the green microalga *Chlorella*
86 *sorokiniana* was cultivated with bacteria. Other studies have also reported that the use of
87 microalgae is an efficient bioremediation strategy for PAH removal, since phototrophs can also
88 co-metabolize PAHs together with bacteria ([Haritash and Kaushik, 2009](#)). Indigenous microalgae-
89 bacteria consortia have effectively been applied in the biodegradation of crude oil and naphthenic
90 acids water ([Tang et al., 2010](#); [Mahdavi et al., 2015](#)). More recently, studies have shown that
91 bacteria associated with microalgae, the phycosphere, could play a significant role in hydrocarbon
92 degradation ([Thompson et al., 2017; 2018](#)). Hence, the phycosphere has attracted considerable
93 interest regarding its potential in pollutant degradation, and scientists have focused on its structure,
94 ecology and interaction with algae. Studies have shown that the bacteria associated with algae,
95 which comprise both algae-attached and free-living bacteria, are specific to algal species, as algae
96 can release strain-dependent organic compounds that are used by specific bacteria ([Bagatini et al.,](#)
97 [2014](#)). The presence of oil- and hydrocarbon-degrading bacteria within the phycosphere has been
98 reported for dinoflagellates and diatoms ([Gutierrez et al., 2012](#); [Mishamandani et al., 2016](#); [Severin](#)
99 [et al., 2016](#); [Thompson et al., 2017, 2018](#)). These associated bacteria can influence the
100 phytoplankton taxon-specific response to hydrocarbon pollution and oil spills ([Severin and Erdner,](#)
101 [2019](#)). Most studies have concerned planktonic microalgae and their associated bacteria, but little
102 is known about the PAH biodegradation potential of microbenthic organisms. Benthic diatoms,
103 thriving in contaminated sediments, can acquire physiological abilities to tolerate and metabolize
104 pollutants ([Kottuparambil and Agusti, 2018](#)).

105 Considering these findings, the present study assessed the role of an indigenous benthic
106 diatom and associated bacteria (co-culture, non-axenic) or benthic diatom alone (axenic culture)
107 in the removal of two PAHs of interest, i.e. BaP and Flt. These two PAHs differ in

108 structure/molecular weight and hydrophobicity/water solubility, leading to potentially different
109 degradation capacities by microalgae and bacteria. Subsequently, the structures of bacteria
110 associated with the diatom (attached or free-living) were also evaluated by Illumina MiSeq 16S
111 rRNA sequencing analysis. Finally, isolated strains from associated bacteria were screened for
112 their potential use of crude oil for growth. The diatom was isolated from a sediment of the Bizerte
113 Lagoon (Tunisia), where high levels of PAHs have been recorded, with Flt and BaP as dominant
114 compounds (265 and 168 $\mu\text{g kg}^{-1}$ dry wt., respectively) (Lafabrie et al., 2013; Pringault et al.,
115 2016). Furthermore, previous works have highlighted that the indigenous microorganisms of the
116 lagoon (bacteria or diatoms) can potentially biodegrade PAHs (Ben Said et al., 2008; Melliti Ben
117 Garali, 2016). Therefore, it seems relevant to evaluate their co-metabolic synergy for a more
118 efficient and faster bioremediation.

119 **2. Material and methods**

120 ***2.1. Microalgae isolation, culture, and identification***

121 An indigenous diatom was isolated from sediment of the Bizerte Lagoon (north of Tunisia)
122 and then cultured according to the protocol described by Lundholm et al. (2011) and slightly
123 modified by Melliti Ben Garali et al. (2016). Sediments were collected using a Van Veen grab
124 (Hydrobios) at a station (37°15'40.22''N and 9°51'30.49''E) located in front of a cement
125 manufactory, which is highly contaminated by PAHs (Lafabrie et al., 2013; Barhoumi et al., 2014).
126 The sediment was sieved through a 2-mm mesh to remove coarse debris. In the laboratory, 3 g of
127 fresh sediment were mixed with 90 mL of a sterilized f/2 hydroponic culture medium (Guillard
128 and Ryther, 1962) and incubated for 6 days in a thermostatic chamber at 22°C, illuminated with
129 cool-white fluorescent tubes at a light intensity of 100 $\mu\text{mole photons m}^{-2} \text{ s}^{-1}$ and under a
130 photoperiod of 12 light: 12 dark. During incubation, the mixture was gently stirred to allow the
131 release of microalgae from the sediments and their recovery to the surface. The supernatant,

132 containing the cells, was taken and served to isolate the dominant diatom. Samples with live cells
133 were examined under an inverted microscope (CETI, Versus, Belgium), and single cells were
134 isolated using a glass Pasteur pipette into a tissue culture plate containing f/2 medium. All cultures
135 were kept under the conditions described previously. The strain was re-inoculated into fresh
136 medium at 2-week intervals. Cells from the culture were observed under a light microscope BX-
137 102. The diatom was identified as a species of *Nitzschia*, based on the morphometric characteristic
138 described by Bouchouicha Smida et al. (2014) (width, length, and form of the valves; number and
139 form of the chloroplasts; presence or absence of the central interspace).

140 **2.2. Sampling of attached and free-living bacteria**

141 To obtain attached bacteria (AB), 200 mL of the *Nitzschia sp.* culture were filtered through a
142 5.0- μm Nuclepore polycarbonate membrane. The free-living bacteria (FB) were recovered by
143 collecting 5.0 μm of the filtrate onto a 0.22- μm cellulose polyester filter. These filters (two filters
144 of 0.5 μm and two filters of 0.22 μm) were used for microbiological and molecular experiments.

145 **2.3. DNA extraction, qPCR quantification, and Illumina Miseq sequencing and analysis**

146 Total DNA was extracted from AB and FB filters (0.5 and 0.22 μm , respectively) using the
147 Ultra Clean Water DNA kit (MO BIO), following the instructions of the manufacturer. The
148 quantification of the DNA obtained and assessment of its purity were performed using the
149 NanoDrop 2000 spectrophotometer (Thermo Scientific, USA).

150 The abundance of total bacteria in AB and FB DNAs was estimated by real-time PCR
151 targeting 16S rRNA genes, using the primer sets 331F/797R. The qPCR was made in triplicate in
152 a Bio-Rad CFX-96 real-time system (Bio-Rad). The reaction components and qPCR protocol
153 conditions have been described previously (Ben Abdallah et al., 2018). The abundance of total
154 bacteria was reported as DNA copy numbers of the corresponding gene per mL, using the standard
155 curves.

156 The AB and FB DNAs samples were subjected to sequencing on an Illumina Miseq platform
157 (CBS, SFAX, TUNISIA), using a paired-end 300-bp sequence read running with the Miseq
158 Reagent Kit V3 (600cycles). The V3-V4 regions of prokaryotic 16S rRNA genes were PCR-
159 amplified with primers Pro341/Pro805R (Takahashi et al., 2014), using KAPA HiFi HotStart
160 ReadyMix (2X) (KAPA Biosystems, Kit Code KK2602). The DNA samples were independently
161 amplified in triplicated 25 µL reactions containing 0.1-10 ng target DNA, 1× Taq PCR Master
162 Mix, and 400 nM of each primer. The PCR program was 30 s at 94°C, 30 s at 55°C, and 45 s at
163 72°C for 30 cycles, followed by 10 min of final primer extension. The products of PCR products
164 were purified using AMPure XP beads (Beckman Coulter, USA) following the manufacturer's
165 recommendations and analyzed with a BioAnalyzer DNA 1000 Chip Kit (Agilent Technologies)
166 and the Qubit® ds DNA HS Assay Kit (Life Technologies). Taxonomic analyses of sequence
167 reads were performed with the QIIME version 1.9.1 software package (Caporaso et al., 2010).
168 Chimera detection was performed with UCHIME, and chimeric sequences were filtered and
169 discarded prior to further analysis (Edgar et al., 2011). Operational taxonomic units (OTUs) were
170 assigned at 97% similarity threshold with the UCLUST algorithm (Edgar, 2010). Taxonomic
171 assignments were performed with the Greengenes 13.8 database. Sequences from selected
172 dominant OTUs (> 1% of all sequences) were compared with related sequences retrieved from
173 NCBI databases using BLAST. The 16S rRNA gene sequences determined in this study were
174 deposited in the GenBank database under accession numbers MT229144 to MT229165.

175 For AB and FB communities, alpha diversity indices including Chao1 richness estimator,
176 observed species and diversity indices (Shannon and Weaver, 1949; Simpson, 1949), as well as
177 the phylogenetic diversity (PD whole-tree) index (Lozupone and Knight, 2008) were calculated
178 with the Qiime software. The VENN DIAGRAM PLOTTER program
179 (<http://omics.pnl.gov/software/VennDiagramPlotter.php>) was used to generate the Venn diagram.

180 ***2.4. Isolation, identification, and screening for bacteria growing on crude oil***

181 **2.4.1. Isolation**

182 In an attempt to isolate strains of attached and free-living bacteria, the filters (5.0 and 0.22
183 μm , respectively) were transferred to sterile tubes containing physiological water (NaCl 9%).
184 Aliquots (100 mL) of serial dilutions were plated onto solid Luria-Bertani as rich medium,
185 containing (per liter): 10 g (w/v) tryptone (Bio Basic, Canada); 5 g (w/v) yeast extract (Panreac,
186 Espagne); 5 g (w/v) NaCl (Bio Basic, Canada), and 20 g (w/v) agar (Bio Basic, Canada). The pH
187 was adjusted to 7 with 10 M KOH before autoclaving. After 1-3 days of incubation at room
188 temperature (approximately 27°C), yellowish, cream, and white colonies were obtained. Different
189 colonies were picked and re-streaked several times to obtain pure cultures and then stored at -80°C
190 in the isolation medium supplemented with 30% glycerol. Cell morphology was observed at 100
191 x magnification under oil immersion (Nikon Optiphot, Tokyo, Japan).

192 **2.4.2. Molecular identification**

193 Genomic DNA of both FB and AB isolates was extracted using a GF1-vivantis Nucleic acid
194 extraction kit according to the manufacturer's protocol. The 16S rRNA genes were amplified using
195 primer sets FD1 (5'- AGAGTTTGATCCTGGCTCAG-3') (Weisburg et al., 1991)/1492R (5'-
196 GGTTACCTTGTTACGACTT-3') (Lane, 1991). The PCR cycling conditions were the same as
197 previously described (Karray et al., 2018). The PCR products were sequenced using the Big Dye®
198 Terminator cycle Sequencing kit and an ABI PRISM 3100 Genetic Analyzer (Applied Biosystems)
199 with FD1 and 1492r primers. Phylogenetic analysis of 16S rRNA gene sequences was performed
200 as previously described (Ben Abdallah et al., 2018). The 16S rRNA gene sequences of the bacterial
201 isolates were deposited in GenBank under accession numbers MN517112 to MN517117.

202 **2.4.3. Screening for bacteria growing on crude oil**

203 The isolated strains were grown aerobically at room temperature in mineral salt medium
204 (MSM) containing (per liter): $(\text{NH}_4)_2\text{SO}_4$, 1g; NaH_2PO_4 , 0.8; K_2HPO_4 , 0.2; MgSO_4 , 0.2; CaCl_2 ,
205 0.1; FeCl_3 , 0.005; MnSO_4 , 0.0002; ZnSO_4 , 0.0001; CuSO_4 , 0.00002; yeast extract, 0.5 g (pH = 7)

206 (Yirui et al., modified 2009). Cells were cultured in 250-mL flasks containing 100 mL of liquid
207 medium with 1 g of crude oil (BAL 150 type Arabian light) for approximately 1 month. A control
208 (without inoculation) was included. Strain evolution was followed by microscopic observation,
209 and their capacity to grow in the presence of crude oil was detected by visual changes in the culture
210 (i.e., clear appearance indicated use of crude oil).

211 ***2.5. PAHs contamination experiment***

212 ***2.5.1. Chemicals and preparation of PAH solution***

213 Two concentrated solutions of BaP and Flt were prepared with HPLC-grade
214 dimethylsulfoxide (DMSO, Sigma Aldrich D4540), and both PAH solutions were kept in the dark
215 at 4°C prior to use. The PAHs (purity > 98%) were purchased from Sigma-Aldrich. Stock solutions
216 of BaP and Flt (0.12 and 2.4 g L⁻¹, respectively) were prepared by dissolving pure chemicals in
217 reagent-grade dimethylsulfoxide (DMSO, 0.05%) without exceeding the solubility threshold.

218 ***2.5.2. Experimental set up***

219 The contamination experiment was conducted under the following conditions: non-axenic,
220 axenic (without bacteria), and sterile (without microorganisms). For the non-axenic condition, nine
221 Erlenmeyer flasks (2 L, Schott-Duran glass), containing 150 mL of exponential diatom culture
222 (initial concentration of 1.1 10⁴ cells mL⁻¹) and fresh f/2 medium, were used to carry out three
223 treatments in triplicate: control treatment without any PAH (treatment C); treatment contaminated
224 with Flt and treatment contaminated with BaP. The Flt and BaP were added to achieve final
225 concentrations of 265 and 3 µg L⁻¹, respectively. These levels were very close to their respective
226 solubility. For the axenic condition, the culture medium was autoclaved and sterilized with a
227 mixture of two antibiotics (10,000 penicillin units and 10 mg of streptomycin per mL, Sigma
228 Aldrich, PO781,) according to the protocol of Réveillon et al. (2016). Then, the three treatments
229 (C, Flt, and BaP) were subjected to the same conditions as the non-axenic treatment. The axenic
230 and non-axenic treatments (C, Flt, and BaP) were incubated for 7 days in a thermostatic chamber

231 under the same conditions used for diatom cultures. The light intensity and the temperature within
232 the incubator were checked throughout the experiment, using a spherical quantum mini-recorder
233 LI-250 A and a thermometer (Model TH-020), respectively. Sterile treatments were performed in
234 triplicates, in which the Erlenmeyer flask contained only f/2 culture medium (for treatment C) and
235 f/2 medium with the PAHs for the treatments Flt and BaP. The sterile treatments were incubated
236 for 7 days in light or in dark and settled to determine PAH removal by abiotic processes, i.e.,
237 photooxidation, volatilization, and adsorption on glass walls (see below).

238 **2.5.3. PAH analysis**

239 The PAHs were analyzed at the beginning and the end of the incubation in axenic and non-
240 axenic cultures as well as in sterile Erlenmeyer flasks in the light and the dark. Sub-samples (100
241 mL) were filtered through precombusted Whatman GF/F filters, and the filtrate and suspended
242 particulate matter (SPM) adsorbed to the filters were used to extract dissolved and particulate
243 PAHs, respectively.

244 Extraction of the SPM-loaded filters was conducted as previously described (Liu et al.,
245 2016), with some modifications. Briefly, after freeze drying and weighing, the filters were spiked
246 with surrogate standard (1-methylpyrene) and ultrasonicated for 1 h at 30°C with 30 mL of a
247 mixture of *n*-hexane:acetone (1:1, v/v). Subsequently, the obtained extract was concentrated to
248 about 5 mL in a rotary evaporator. Additional 10 mL of *n*-hexane were added to the pear-shaped
249 flask and evaporated down to few hundreds of μ L. This concentrated extract was purified through
250 a glass column packed with 1 g anhydrous sodium sulfate in the upper part and 2 g of silica gel
251 (previously activated by heating at 150°C overnight before use) in the lower part. After
252 conditioning with 8 mL of *n*-hexane, the fraction containing PAHs (Flt and BaP) was eluted with
253 10 mL of the mixture of *n*-hexane and dichloromethane (1:1, v/v). The eluents were concentrated
254 to 1-2 mL, subjected to solvent exchange to acetonitrile, and concentrated to 1.0 mL by a rotary

255 evaporator prior to HPLC analysis. Extraction of dissolved PAHs was performed by Liquid-
256 Liquid extraction (LLE) with 15 mL of dichloromethane (DCM) for 5 min. The extraction was
257 repeated three times, and the obtained extracts were combined. The subsequent steps were identical
258 as those described for SPM-loaded filter pretreatment.

259 Quantification of Flt and BaP was conducted using an analytical HPLC unit (JASCO, Japan)
260 equipped with a JASCO PU-2089 HPLC pump, a type 7125 Rheodyne injector (with a 20 μ L
261 loop), and a fluorescence detector (FP-2020) with excitation and emission wavelengths that could
262 be varied throughout the analysis (Ex/Em: 288/462 nm (Flt), Ex/Em: 290/430 nm (BaP)).
263 Separation was carried out using a SUPELCOSIL LC-PAH (Supelco, Inc. Bellefonte, PA) reverse-
264 phase C18 column (4.6 \times 250 mm, 5 μ m particle size) specific for PAH analysis. Acetonitrile was
265 used as mobile phase (isocratic elution mode), operated at a flow rate of 1 mL min⁻¹; injection
266 volume was 20 μ L. We identified Flt and BaP via comparison of their retention time with those of
267 the authentic standards and quantified them using the internal calibration method.

268 All data were subjected to strict quality control procedures. A series of solvent blanks (to
269 determine any background contamination), spiked blanks, and a spiked matrix (to monitor
270 recovery efficiency) were analyzed during the treatment and analysis procedures. Solvent blanks
271 showed that Flt and BaP were detected in small amounts (< 5% of sample values). The spiked
272 recoveries of Flt and BaP in water and filters were set in the range 82.3-100.6% and 95.7-113.3%.
273 Method detection limits (MDLs), defined as mean blank value + 3 \times standard deviation (SD),
274 ranged from 0.02 to 0.10 ng mL⁻¹ in water and filters. The concentrations of Flt and BaP were
275 blank corrected, but not corrected with recoveries. All solvents used for sample processing and
276 analyses (DCM, hexane, acetone, and acetonitrile) were of high-performance liquid
277 chromatography (HPLC) grade and were purchased from Fisher (UK). All glassware was
278 intensively cleaned before using.

279 **2.5.4. Chl *a* analyies**

280 Subsamples (50 mL) from axenic and non-axenic cultures were taken daily and filtered
281 through glass microfiber filters (GF/F, Whatman). The Chl *a* was extracted with 90% acetone (v/v)
282 for 30 h in the dark at 5°C. The pigment concentration was measured using the spectrophotometric
283 method provided by Lorenzen and Jefferey (1980), following the procedure described in Parsons
284 et al. (1984).

285 **2.5.5. Growth kinetics**

286 To determine the diatom growth kinetics, subsamples (1 mL), taken daily from replicates of
287 axenic and non-axenic treatments, were fixed with Lugol's acid solution (3% final concentration).
288 Cell counting was performed in triplicate on aliquots of 5 µl, deposited between slide-coverslip
289 and observed under a light microscope BX-102 A at × 40 magnification (Lundholm et al., 2004).
290 The exponential growth rate was calculated by considering three successive counts made in the
291 exponential growth phase, according to the formula $N_t = N_0 e^{\mu t}$ and $\ln(N_t / N_0) = \mu t$, where N_0
292 and N_t are the initial and final abundance values of the diatom, respectively; μ (d^{-1}) is the net cell
293 growth rate; t (d) is the incubation time; μ is the slope of the line from the linear regression of \ln
294 (N_t / N_0) against time of the form $y = a x$.

295 **2.5.6. Bacterial monitoring in axenic cultures**

296 To ensure the success of the axenization method, total bacteria were enumerated via real-
297 time PCR targeting 16S rRNA genes, using the primer sets 331F/797R as described above
298 (Paragraph 2.3). Subsamples were collected from axenic cultures at the beginning of the
299 experiments and after 3 and 7 days. Subsamples (200 mL) were filtered (0.5 and 0.22 µm), and
300 total DNA was extracted from filters as described in Paragraph 2.3.

301 **2.6. Determination of the relative contribution of the different PAH removal processes**

302 The percentages of dissolved PAHs (i.e., in the medium, %PAH_{dis}), accumulated in the cells
303 (%PAH_{acc}), and degraded (%PAH_{deg}) were calculated as follows (Chan et al., 2006):

$$304 \quad \%PAH_{dis} = C_{PAH_{dis}} / C_{PAH_{initial}} \times 100$$

305 $\%PAH_{acc} = C_{PAH_{part}} / C_{PAH_{initial}} \times 100$

306 $\%PAH_{deg} = (C_{PAH_{initial}} - C_{PAH_{dis}} - C_{PAH_{part}}) \times 100,$

307 where $C_{PAH_{initial}}$ represents the amount of PAHs added at the beginning of the incubation and
308 $C_{PAH_{dis}}$ and $C_{PAH_{part}}$ represent the amounts of PAHs measured at the end in the dissolved and
309 particular fractions, respectively.

310 Many processes could contribute to the degradation of PAHs during the incubation. The
311 main abiotic process is photodegradation (PAH_{pho}), but volatilization (PAH_{vol}) and adsorption on
312 the walls of the glass bottles (PAH_{ads}) may also lead to PAH decrease and were therefore
313 considered in the calculation. The biotic processes were assigned to the biodegradation by
314 microorganisms (PAH_{biodeg}), including diatoms (PAH_{diadeg}) and total bacteria (PAH_{bacdeg}). The
315 importance of these processes is expected to differ among the experimental conditions, and hence,
316 the percentage of degraded PAHs is likely to vary:

317

318 *Sterile condition*

319 *in the dark:* $\%PAH_{deg} = \%PAH_{vol} + \%PAH_{ads}$ (Eq. 1)

320 *in the light:* $\%PAH_{deg} = \%PAH_{vol} + \%PAH_{ads} + \%PAH_{pho}$ (Eq. 2)

321 So, Eq2 - Eq1 = $\%PAH_{pho}$

322 The $\%PAH_{vol} + \%PAH_{ads}$ and $\%PAH_{pho}$ were considered as equivalent for all treatments and conditions.

323

324 *Axenic condition*

325 $\%PAH_{deg} = \%PAH_{vol} + \%PAH_{ads} + \%PAH_{pho} + \%PAH_{biodeg}$ (Eq. 3)

326 Therefore, Eq3 - Eq2 = $\%PAH_{biodeg}$

327 In axenic cultures, biodegradation was due to the diatom, and therefore, the $\%PAH_{biodeg}$ was equal to
328 the $\%PAH_{diadeg}$, which would not differ considerably from that of the non-axenic culture.

329

330 *Non-axenic condition*

331 $\%PAH_{deg} = \%PAH_{vol} + \%PAH_{ads} + \%PAH_{pho} + \%PAH_{biodeg}$ (Eq. 4)

332 Therefore, Eq4 - Eq2 = $\%PAH_{biodeg}$

333 In non-axenic cultures, biodegradation was due to both diatom biodegradation and bacterial
334 biodegradation; therefore, the $\%PAH_{biodeg}$ minus the $\%PAH_{diadeg}$ equaled to $\%PAH_{bacdeg}$.

335

336

337 *2.7. Statistical analysis*

338 Statistical analyses were performed using the SPSS software version 14.0 for Windows.
339 Analysis of variance (ANOVA) was used to test the effects of BaP and Flt on Chl *a*, cell density,
340 and growth rate. When the effect was significant, a multiple comparison posterior test (Tukey's
341 test) was performed to compare treatments in a 2 x 2 design. When the normality of data
342 distribution (test of Kolmogorov-Smirnov) and/or the homogeneity of the variances (Bartlett-Box
343 test) could not be verified, a non-parametric ANOVA (Kuskal-Wallis) was used. A student test
344 was performed to compare the fractions of PAH remaining, accumulated, and degraded between
345 axenic and non-axenic conditions and the fraction of PAHs degraded by diatoms and bacteria.

346 **3. Results**

347 **3.1. Responses of *Nitzschia sp.* to BaP and Flt**

348 The diatom maintained in the non-axenic control showed a pronounced growth, as the Chl
349 *a* concentration increased significantly from an initial value of 37 ± 2.6 to $177 \pm 19.5 \mu\text{g L}^{-1}$ at the
350 end of the experiment (Fig. 1a). In BaP and Flt treatments, Chl *a* also showed an increase
351 throughout the incubation, with slightly lower concentrations at the end of the experimental period
352 ($134 - 137 \pm 10.5 - 19.5 \mu\text{g L}^{-1}$) relative to the control (Fig. 1a). In non-axenic cultures, the overall
353 effect of the two PAHs on biomass was not significant ($P > 0.05$). In the control, *Nitzschia sp.*
354 exhibited a growth kinetics characterized by a 2-day latency, followed by exponential growth until
355 the end of the incubation period, where it reached extremely high densities ($31 \pm 5.2 \cdot 10^4 \text{ cells mL}^{-1}$)
356 (Fig. 1b). In both PAH treatments, the diatom showed the same pattern of proliferation; growth
357 rates ($0.44 \pm 0.009 \text{ d}^{-1}$ and $0.45 \pm 0.0003 \text{ d}^{-1}$) were not significantly different from those of the
358 control ($0.50 \pm 0.01 \text{ d}^{-1}$) ($P > 0.05$, Table 1).

359 The axenization of the diatom was successfully maintained during the experiment, as no
360 bacterial abundance was detected by qPCR throughout the incubation period. The axenic strain of
361 *Nitzschia sp.* showed continuous proliferation in the control, with Chl *a* concentrations ($18 -$
362 $92 \mu\text{g L}^{-1}$) and cell density levels ($0.75 - 17 \cdot 10^4 \text{ cells mL}^{-1}$) significantly lower than those in the non-

363 axenic control ($37\text{-}177 \mu\text{g Chl } a \text{ L}^{-1}$; $1\text{-}31 \cdot 10^4 \text{ cells mL}^{-1}$), concomitant with the lower growth rate
364 (Table 1). Contamination with Flt caused a slight decrease in cell density (Fig. 2d), but the growth
365 rate remained similar ($0.41 \pm 0.016 \text{ d}^{-1}$) to that of the control ($0.43 \pm 0.03 \text{ d}^{-1}$) (Table 1). In contrast,
366 BaP addition provoked a significant decrease in Chl *a* and cell density (Fig. 1c, d), together with
367 a decrease in growth rate ($0.35 \pm 0.002 \text{ d}^{-1}$) relative to the control (Table 1). When comparing the
368 responses of the axenic and non-axenic diatom strains, the most pronounced decrease induced by
369 PAHs (especially for BaP) on *Nitzschia* growth was observed in the axenic culture.

370 **3.2. Fate of BaP and Flt**

371 The concentrations of Flt and BaP, measured in each treatment at the beginning of the
372 experiment, were compared with those used theoretically for contamination (Table 2). The results
373 show that the measured levels were close to 95% of the theoretical concentrations. Therefore, the
374 measured concentrations were used in the remainder of the results.

375 For all treatments and conditions, PAH levels remaining at the end of the experiment were
376 low (maximum $8.5 \pm 1.4\%$ for BaP). In contrast, PAH degradation (%PAH_{deg}) and PAH
377 accumulation in the cells (%PAH_{acc}) were the dominant processes involved in PAH removal
378 (Table 3). However, the %PAH_{acc} and %PAH_{deg} were significantly different between non-axenic
379 and axenic cultures ($P < 0.05$, Table 3). There was more PAH accumulated in the axenic culture
380 ($52.8\% \pm 3.0\%$ for BaP and $33\% \pm 2.0\%$ for Flt) than in the non-axenic culture ($18.1 \pm 1.6\%$ for
381 BaP and $11.3 \pm 1.5\%$ for Flt). Conversely, the highest degradation was observed in non-axenic
382 cultures for both BaP and Flt ($79.4 \pm 2.3\%$ and $88.2 \pm 4.2\%$, respectively). Interestingly, the abiotic
383 removal of PAHs, mainly due to the photooxidation, did not account for more than $10 \pm 1.8\%$ for
384 BaP and $7.9 \pm 1.1\%$ for Flt. Hence, biodegradation was generally the main process of PAH
385 removal. Biodegradation of Flt was higher than that of BaP under both conditions, while more BaP
386 was accumulated. Interestingly, significant differences ($P < 0.05$) were observed for bacterial and
387 diatom degradation between both PAHs. Bacteria were able to degrade $40.7 \pm 2.5\%$ of the initial

388 BaP concentration, whereas the diatom showed a lower ability to degrade this PAH ($28.7 \pm 2.6\%$).
389 In contrast, the microalgae exhibited a high degradation of Flt ($53.5 \pm 3.2\%$) compared to the
390 bacteria ($26.8 \pm 2.2\%$). Moreover, the degradation level of Flt by the diatom was significantly (P
391 < 0.05) larger than that of BaP.

392 ***3.3. Diversity and abundance of attached and free-living bacteria communities associated to*** 393 ***Nitzschia sp.*** 394

395 The diversity of attached (AB) and free-living bacteria (FB) associated to *Nitzschia sp.* was
396 evaluated using the 16S rRNA gene high-throughput sequencing approach. To identify and
397 compare both AB and FB diversity, sequences were analyzed under the same conditions. Overall,
398 865 different OTUs were detected in the prokaryotic communities associated to the *Nitzschia sp.*
399 culture. However, the AB community displayed higher species richness (observed OTUs) (562
400 OTUs) and species diversity (Simpson, Shannon indices) than the FB community (303 OTUs)
401 (Table 4). In addition, the average abundance of free-living cells was lower ($0.34 \pm 0.06 \times 10^5$
402 DNA copies ml^{-1}) than that of attached bacteria ($2.1 \pm 0.42 \times 10^5$ DNA copies mL^{-1}).

403 Analysis of AB community composition showed that Alphaproteobacteria (54.0%),
404 Cyanobacteria (35.5%), Bacteroidetes (3.4%), Gammaproteobacteria (3.3%), and Planctomycetes
405 (2.7%) dominated the bacterial communities (Fig. 2a). The FB were greatly dominated by
406 Alphaproteobacteria (51.9%), followed by Bacteroidetes (36.6%), Betaproteobacteria (4.8%),
407 Firmicutes (2.0%), and Planctomycetes (1.2%). Within the archaea domain, Euryarchaeota was
408 exclusively presented at low abundance (0.25%) in the AB fraction (Fig. 2a). Alphaproteobacteria
409 (representing more than half of the prokaryote communities) and Planctomycetes (found in lower
410 proportion) were observed in both AB and FB fractions. Actinobacteria, Betaproteobacteria, and
411 Firmicutes were typically found among the FB fraction, while Cyanobacteria and
412 Gammaproteobacteria were exclusively found among the attached bacteria, while Bacteroidetes
413 were more abundant in the FB fraction than in the AB sample.

414 A Venn diagram demonstrated that OTUs differed among AB and FB fractions (Fig. 2c). In
415 total, 217 OTUs were shared between both samples. A larger number of specific OTUs was
416 detected in the AB fraction (345 OTUs) than in the FB fraction (86 OTUs). However, AB and FB
417 were only dominated by 12 and 14 OTUs, respectively (Table S1). To further analyze the microbial
418 community composition and structure, dominant genera (> 1% of all sequences) are presented in
419 Fig. 2b. The most abundant genera, namely *Phaeocystidibacter*, *Mabikibacter*, *Roseitalea*,
420 *Nioella*, and *Erythrobacter*, were identified in both AB and FL fractions. The genera
421 *Dulcicalothrix*, *Chamaesiphon*, *Roseimaritima*, *Oricola*, and *Aestuariibius* were greatly related to
422 the AB fraction. The FB fraction was particularly dominated by a member of the family
423 Cryomorpaceae, previously isolated from marine algae (35.5% of all sequences), followed by the
424 genera *Agrococcus*, *Pyruvatibacter*, *Acuticoccus*, *Marivita*, *Roseibaca*, and *Alcaligenes*.

425 **3.4. Morphological characterization of bacterial isolates**

426 Based on the morphological characteristics of the colonies, six bacterial strains from diatom
427 *Nitzschia sp.* pure cultures were isolated and tested for their growth on crude oil (Table 5). Five
428 strains (2, 3, 4, 5, and 6) belonged to the FB fraction, while Strain 1 was obtained from the AB
429 fraction. Colonies were small, large, circular, round, smooth, oval, and approximately between
430 0.05 and 5 μm of diameter. Among these colonies, three strains (1, 2, 6) forming cream-colored
431 colonies were obtained. Other colonies were yellow (Strain 3), white (Strain 4), and transparent
432 (Strain 5). Cells of aerobic isolates were long rods (3-6 μm long x 0.1 μm wide) or coccoid (0.2-
433 0.5 μm size), occurring as single cells or in pairs.

434 **3.5. Phylogenetic analysis of attached and free-living bacterial isolates**

435 The 16S rRNA gene sequences from the six strains were generated to determine their
436 taxonomic group. Phylogenetic analysis revealed that those isolates belonged to the three phyla:
437 *Proteobacteria* (*Gammaproteobacteria* class), *Firmicutes*, and *Actinobacteria* (Fig. 3). Strains 1
438 (attached bacteria), 4, and 6 (free-living bacteria) were related to the genus *Staphylococcus*. The

439 free-living bacterial Strains 2 and 3 belonged to *Acinetobacter* and *Micrococcus*, respectively.
440 Strain 5 was affiliated to the species *Bacillus amyloliquefaciens*. These bacterial taxa showed low
441 abundances (< 0.5% of all sequences) in both AB and FB fractions.

442 **3.6. Screening for bacteria growing on crude oil**

443 Following isolation and purification, all selected strains were screened for their potential
444 growth in the presence of crude oil. After 15 days of incubation, there was a visual change in the
445 aspect of oil crude with Strains 3, 4, and 6. After 30 days, microscopic observation showed that
446 cultures of these strains had a clear appearance and a turbid aspect, suggesting that Strains 3, 4,
447 and 6 (belonging to the genera *Micrococcus* and *Staphylococcus*) could maintain their growth in
448 the presence of crude oil under aerobic conditions (Table 5).

449 **4. Discussion**

450 **4.1. Influence of the associated bacteria on *Nitzschia* growth**

451 In comparison to the axenic condition, *Nitzschia sp.* exhibited higher growth in non-axenic
452 cultures (Table 1), with higher biomass and cell density (Fig. 1). This result agrees with previous
453 findings that the presence of bacteria can promote the proliferation of microalgae (Kazamia et al.,
454 2012; Amin et al., 2015). A commonly studied interaction between microalgae and their associated
455 bacteria is the bacterial production of vitamins (cobalamin, thiamine, and biotin) required by algal
456 species for their growth (Kazamia et al., 2012). Diatom growth can also stimulated by bacteria
457 (mainly *Proteobacteria*) through the excretion of extracellular polysaccharides (EPS) by
458 phototrophs. These EPS, after bacterial remineralization, constitute an important nutrient source
459 (Bruckner et al., 2008). Other studies also reported that the bacterial presence is beneficial for
460 diatoms through the secretion of extracellular indole acetic acid (IAA), which is an auxin that
461 optimizes algal growth (Seyedsayamdost et al., 2011; Lépinay et al., 2018). Amin et al. (2015)

462 showed that *Sulfitobacter* species could favor the division of the diatom *Pseudonitzschia*
463 *multiseriis* via the production of IAA by using the diatom's secreted and endogenous tryptophan.

464 **4.2. Tolerance of *Nitzschia sp.* to PAHs**

465 In this study, *Nitzschia sp.* was exposed to high levels of PAHs (256 $\mu\text{g Flt L}^{-1}$ and 3 $\mu\text{g BaP}$
466 L^{-1}), which exceeded the EC50 of growth inhibition reported for diatoms (18-200 $\mu\text{g L}^{-1}$ for Flt
467 and 1.18 $\mu\text{g L}^{-1}$ for BaP) (Liu et al., 2006; Niehus et al., 2018). Despite this, the diatom kept a
468 continuous proliferation until the end of the incubation in both axenic and non-axenic conditions
469 (Fig. 1). In some case, biomass and cell density in contaminated cultures were lower than in the
470 control, but growth rates were not significantly different, except for BaP in the axenic culture
471 (Table 1; Fig. 1). This indicates that *Nitzschia sp.* can tolerate both HAPs; this is in agreement with
472 the study of Croxton et al. (2015), who showed that the growth of *Nitzschia brevis* was
473 unaffected by high a concentration of naphthalene (1,000 $\mu\text{g L}^{-1}$). Nevertheless, other studies have
474 observed a significant decrease in diatom growth after PAH exposition (Bopp and Lettieri, 2007;
475 Niehus et al., 2018). Obviously, the degree of tolerance/sensitivity to pollutants varies among algal
476 species and depends greatly on the environment in which microalgae evolve (Ben Othmen et al.,
477 2018; Pikula et al., 2019). According to Kottuparambil and Agusti (2018), microalgae, via natural
478 evolution, can gain higher resistance to pollutants, allowing the survival of their populations in
479 highly polluted environments. Consequently, *Nitzschia sp.*, isolated from a PAH-contaminated
480 sediment of the Bizerte Lagoon (LaFabrie et al., 2013; Pringault et al., 2016), seems to be
481 accustomed to high levels of PAHs and has acquired physiological abilities to tolerate and even
482 metabolize these pollutants. This is in line with the idea that several diatom species were identified
483 as good indicators of high PAH levels in surface sediments (Potapova et al., 2016). Interestingly,
484 in PAH treatments, especially for BaP, *Nitzschia sp.* growth rates were lower in axenic conditions
485 compared to non-axenic ones (Table 1, Fig. 1). This suggests that the presence of bacteria was
486 beneficial for the diatom by improving its capacity to tolerate PAHs, which leads us to infer that

487 associated bacteria could protect the microalgae by reducing PAH toxicity, as has been observed
488 for metals and pesticides (Fouilland et al., 2018) or tannic acid (Bauer et al., 2010).

489 **4.3. PAH accumulation and biodegradation**

490 The PAH concentration in the dissolved fraction was extremely low at the end of the
491 incubation, as the amounts of BaP and Flt remaining in the medium did not exceed 2.5-8.5 and
492 0.5-5.6%, respectively (Table 3). Several processes, including abiotic and biotic factors, can
493 contribute to PAH elimination (Ghosal et al., 2016). Abiotic losses, mainly due to photooxidation,
494 did not account for more than 10%. This indicates the high capacity of microorganisms to eliminate
495 PAHs, which is in agreement with previous studies reporting that a large fraction of PAH removal
496 in microalgae culture was attributed to biotic degradation (Hong et al., 2008; Diaz et al., 2015;
497 Kumari et al., 2016; García et al., 2017).

498 The amounts of PAHs biodegraded by *Nitzschia sp.* alone (28.7-53.7%) were 1.5-2.4 times
499 lower than when bacteria were present (69.4-80.3%) (Table 3). This suggests co-metabolic
500 synergy between microalgae and bacteria in the removal of PAHs, as previously reported (Borde
501 et al., 2003; Coulon et al., 2012, Kumari et al., 2016). The known hydrocarbon-degrading genera
502 *Marivita*, *Erythrobacter*, and *Alcaligenes* (Fig. 2b) and strains growing on crude oil (Table 3) were
503 observed in the bacterial community associated to *Nitzschia*. This suggests that these associated
504 hydrocarbonoclastic bacteria may enhance biodegradation of PAHs in non-axenic cultures, as
505 previously highlighted (Mishamandani et al., 2016; Thompson et al., 2017, 2018; Severin and
506 Erdner, 2019). The degradation of PAHs by microorganisms depends on their molecular weight,
507 hydrophobicity, and water solubility (Haritash and Kaushik, 2009). In general, PAHs with lower
508 molecular weights, lower octanol-water partitioning coefficients (K_{ow}), and higher water solubility
509 are more susceptible to biodegradation. The Flt (four-ring compound) displays a lower molecular
510 weight, a lower log K_{ow} , and a higher water solubility compared to the five-ring BaP (154 vs.
511 252 g mol⁻¹, 5.2 vs. 6, and 240 vs. 1.5 µg L⁻¹, respectively). Biodegradation of Flt by *Nitzschia sp.*

512 (53.5%) was higher than that of BaP (28.7%), whereas a higher proportion of BaP remained
513 accumulated in the diatom, as estimated by the PAH concentration measured in the particular phase
514 (Table 3). This suggests that Flt was more easily metabolized by *Nitzschia sp.* than BaP, which
515 appeared to be more stable and more difficult to degrade. However, in the non-axenic culture,
516 bacterial degradation of BaP (40.7%) was greater than that of Flt (26.8%). Indeed, a bacterial
517 consortium has previously been shown to prefer degrading five-to-six-ring PAHs (Moscoso et al.,
518 2012; Pugazhendi et al., 2016).

519 The accumulation of PAHs by the diatom also contributed to their removal, with %PAH_{acc}
520 varying from 11.3 to 52.8 (Table 3). This is in agreement with previous reports for PAH
521 accumulation by microorganisms, including diatoms (such as *Skeletonema costatum*, *Nitzschia sp.*,
522 *Pseudonitzschia spp.*) (Lei et al., 2007; Hong et al., 2008). The %PAH_{acc} values were higher in
523 axenic (52.8% for BaP and 33% for Flt) than in non-axenic cultures (18.1% for BaP and 11.3%
524 for Flt) (Table 3). The bioaccumulation of PAHs by microalgae is directly related to the size and
525 the morphology of cells as well as the initial cell inoculum (Chan et al., 2006). In our experiment,
526 the same isolate of *Nitzschia sp.* was used in both axenic and non-axenic cultures with similar
527 inoculum densities. However, in the non-axenic culture, bacteria were able to degrade BaP and Flt
528 during the incubation, thereby decreasing the amount of PAH that might be accumulated in the
529 diatom cells (Table 3). Besides their degradation, associated bacteria might also influence the
530 availability of BaP and Flt for the diatom through the production of refractory/hydrophobic
531 dissolved organic matter (DOM). Heterotrophic bacteria are known to produce refractory DOM
532 via the assimilation of freshly produced/labile phytoplankton DOM (Jiao et al., 2010; Moran et al.,
533 2016). This bacteria-derived DOM, more aromatic/hydrophobic, could in turn bind with Flt and
534 BaP through hydrophobic interactions. These DOM-PAHs complexes are larger and more polar
535 than the free dissolved PAHs, thereby decreasing their availability for the diatom (Mei et al., 2009;
536 Yang et al., 2016). The capacity of bacteria associated to *Nitzschia sp.* in reducing PAH

537 accumulation in the diatom and their potential effect on microalgal metabolism may enable the
538 diatom to cope with PAHs, resulting in better growth in non-axenic cultures compared to axenic
539 ones (Table 3, Fig. 1).

540 ***4.4. Composition of associated bacterial communities and hydrocarbonoclastic potential of*** 541 ***bacterial strains***

542

543 There was a difference in community structure between attached (AB) and free-living (FB)
544 bacteria associated to *Nitzschia sp.*; the AB community exhibited a higher diversity and abundance
545 than the FB community. Additionally, a significant variation in the relative abundance between
546 attached and free-living communities was observed (Table 4, Fig. 2). Many studies indicated
547 prominent differences in the community composition of particle-attached and free-living bacteria
548 (Grossart et al., 2005; Bagatini et al., 2014; Rieck et al., 2015). The structure of the bacterial
549 community in the phycosphere, both attached and free-living, is specific to algal species, since
550 algae can release strain-dependent organic compounds that are used by specific bacteria (Bagatini
551 et al., 2014). In this sense, the difference between *Nitzschia*-AB and FB could be explained by the
552 consistent associations between specific bacterial taxa and the *Nitzschia sp.* host (Amin et al.,
553 2012; Sison-Mangus et al., 2014; Behringer et al., 2018). Our results revealed that *Nitzschia*-
554 attached bacteria mainly belonged to Proteobacteria (i.e., Alphaproteobacteria) and Cyanobacteria
555 (Fig. 2a). Previous studies have indicated that Proteobacteria are commonly associated to benthic
556 diatom species (Jaufrais et al., 2017; Keodoodor et al., 2019), and autotrophic nitrogen-fixing
557 bacteria (*Cyanobacteria*) are known to interact with diatoms (Amin et al., 2012).
558 Alphaproteobacteria also predominated in the FB community of *Nitzschia sp.*, as reported
559 previously (Grossart et al., 2005; Buchan et al., 2014). Bacteroidetes, known as a common
560 bacterial phylum associated to diatoms (Grossart et al., 2005; Amin et al., 2012; Jaufrais et al.,
561 2017; Keodoodor et al., 2019), formed a large fraction of the FB of *Nitzschia sp.* (Fig. 2a). Attached
562 and free-living communities were dominated by 16 genera (Fig. 2b), many of which are commonly

563 being observed in algal cultures or as epibionts in several phycospheres of dinoflagellates, diatoms,
564 and coccolithophores (Foster et al., 2011; Wang et al., 2016).

565 The genera *Marivita*, *Erythrobacter*, and *Alcaligenes*, mainly found in the FB community
566 (Fig. 2b), degrade a wide range of xenobiotics, including aliphatic and polyaromatic hydrocarbons
567 (Yuan et al., 2015; Durán et al., 2019; Severin and Erdner, 2019). Furthermore, Strains 3, 4, and
568 6, isolated from the associated bacterial community, were able to grow in the presence of crude oil
569 (Table 5), suggesting the development of oil degraders in the bacterial community associated to
570 the diatom. Our result corroborated with previous reports on the presence of oil-degrading bacteria
571 in some microalgae phycospheres (Mishamandani et al., 2015; Severin et al., 2016; Thompson et
572 al., 2017, 2018). Strains 3, 4, and 6 were related to the genera *Staphylococcus* and *Micrococcus*,
573 which have previously been identified as PAH degraders (Dong et al., 2015; Ghosal et al., 2016;
574 Alegbeleye et al., 2017). Furthermore, species of *Micrococcus* and *Staphylococcus*, isolated from
575 contaminated marine sediments, have been identified as naphthalene-degraders (Melcher et al.,
576 2002; Zhuang et al., 2003) and as biosurfactant producers (Ibrahim et al., 2013; Bao et al., 2014;
577 San et al., 2015). Although associated bacterial communities are generally species-dependent, they
578 can also be influenced by environmental conditions. The benthic *Nitzschia sp.*, used in our study,
579 thrives in PAH-contaminated sediments (LaFabrie et al., 2013; Pringault et al., 2016), conditions
580 that favor the presence of hydrocarbonoclastic bacteria (Ben Said et al., 2008) that might be in
581 close interactions with the benthic diatom. The phycosphere of *Nitzschia sp.* could have contained
582 hydrocarbonoclastic bacteria (mainly in the FB fraction), which could play an important role in
583 the strong biodegradation of Flt and BaP under non-axenic conditions (Table 3).

584 **5. Conclusions**

585 The biodegradation, the most significant process of PAH removal, was significantly higher
586 when bacteria were present in the culture of the benthic diatom (*Nitzschia sp.*). This highlights a
587 possible co-metabolic synergy between microalgae and bacteria in PAH biodegradation, allowing

588 potential bioremediation applications for the removal of PAHs from marine environments.
589 Investigation of the structure of bacterial communities associated to *Nitzschia sp.* (the
590 phycosphere) revealed the possible presence of hydrocarbon-degrading bacteria belonging to the
591 genera *Marivita*, *Erythrobacter*, and *Alcaligenes*. Furthermore, the associated bacteria harbored
592 some strains, assigned to *Staphylococcus* and *Micrococcus*, which were able to grow on crude oil.
593 This indigenous diatom, with its associated hydrocarbonoclastic bacteria, could find an interesting
594 application in environmental biotechnology, enhancing the bioremediation of PAH-contaminated
595 sites, or in depollution strategies following oil spills.

596 **Acknowledgements**

597 This work was supported by IRD through the Laboratoire Mixte International (LMI)
598 COSYS-Med (Contaminants et Ecosystèmes Sud Méditerranéens). English grammar and syntax
599 of the manuscript were revised by Proof-Reading-Service.com.

600 **References**

- 601 [Alegbeleye, O.O., Opeolu, B.O., Jackson, V., 2017. Bioremediation of polycyclic aromatic](#)
602 [hydrocarbon \(PAH\) compounds: \(acenaphthene and fluorene\) in water using indigenous](#)
603 [bacterial species isolated from the Diep and Plankenburg rivers, Western Cape, South Africa.](#)
604 [Braz. J. Microbiol. 48, 314–325](#)
- 605 [Amin, S.A., Parker, M.S., Ambrust, E.V., 2012. Interactions between diatoms and bacteria.](#)
606 [Microbiol. Mol. Biol. Rev. 76, 667–684](#)
- 607 [Amin, S.A., Hmelo, L.R., van Tol, H.M. Durham, B.P., Carlson, L.T., Heal, K.R., Morales, R.L.,](#)
608 [Berthiaume, C.T. Parker, M.S., Djunaedi, B., Ingalls, A.E., Parsek, M.R., Moran, M.A.,](#)
609 [Armbrust, E.V., 2015. Interaction and signalling between a cosmopolitan phytoplankton and](#)
610 [associated bacteria. Nature. 522, 98–101.](#)
- 611 [Arulazhagan, P., Vasudevan, N., 2009. Role of a moderately halophilic bacterial consortium in the](#)
612 [biodegradation of polyaromatic hydrocarbons. Mar. Poll. Bull. 58, 256–262.](#)
- 613 [Bagatini, I. L., Eiler, A., Bertilsson, S., Klaveness, D., Tessarolli, L.P., and Vieira, A.A.H., 2014.](#)
614 [Host-specificity and dynamics in bacterial communities associated with bloom-forming](#)
615 [freshwater phytoplankton. PLoS ONE 9: e85950. doi: 10.1371/journal.pone.0085950](#)
- 616 [Bao, M., Pi, Y., Wang, L., Sun, P., Li, Y., Cao, L., 2014. Lipopeptide biosurfactant production](#)
617 [bacteria *Acinetobacter sp.* D3-2 and its biodegradation of crude oil. Environ. Sci. Process.](#)
618 [Impacts. 16, 897–903](#)
- 619 [Barhoumi, B., Le Menach, K., Devier, M.-H., Ameer, W.B., Etcheber, H., Budzinski, H., Cachot,](#)
620 [J., Driss, M.R., 2014. Polycyclic aromatic hydrocarbons \(PAHs\) in surface sediments from](#)
621 [the Bizerte lagoon, Tunisia: levels, sources and toxicological significance. Environ. Monit.](#)
622 [Assess. 186, 2653–2669.](#)

- 623 Bauer, N., Grossart, H., Hilt, S., 2010. Effects of bacterial communities on the sensitivity of the
624 phytoplankton *Stephanodiscus minutulus* and *Desmodesmus armatus* to tannic acid. *Aquat.*
625 *Microb. Ecol.* 59, 295–306.
- 626 Behringer, G., Ochsenkühn, M.A., Fei, C., Fanning, J., Koester, J.A., Amin, S.A., 2018. Bacterial
627 communities of diatoms display strong conservation across strains and time. *Front. Microbiol.*
628 9, 659. 10.3389/fmicb.2018.00659
- 629 Ben Abdallah, M., Karray, F., Kallel, N., Armougom, F., Mhiri, N., Quéméneur, M., Cayol, J.L.,
630 Erauso, G., Sayadi, S. 2018. Abundance and diversity of prokaryotes in ephemeral hypersaline
631 lake Chott El Jerid using Illumina Miseq sequencing, DGGE and qPCR assays.
632 *Extremophiles.* 22, 811–823.
- 633 Ben Othman, H., Lanouguère, E., Got, P., Sakka Hlaili, A., Leboulanger, C., 2018. Structural and
634 functional responses of coastal marine phytoplankton communities to PAH mixtures.
635 *Chemosphere.* 209, 908-919.
- 636 Ben Said, O., Goni-Urriza, M.S., El Bour, M., Dellali, M., Aissa, P., Duran, R., 2008.
637 Characterization of aerobic polycyclic aromatic hydrocarbon-degrading bacteria from
638 Bizerte lagoon sediments, Tunisia. *J. Appl. Microbiol.* 104, 987–997.
- 639 Bopp, S., Lettieri, T., 2007. Gene regulation in the marine diatom *Thalassiosira pseudonana* upon
640 exposure to polycyclic aromatic hydrocarbons (PAHs). *Gene.* 396, 293–302.
- 641 Borde, X., Guieysse, B., Delgado, O., Munoz, R., Hatti-Kaul, R., Nugier-Chauvin, C., 2003.
642 Synergistic relationships in algal-bacterial microcosms for the treatment of aromatic
643 pollutants. *Bioresour. Technol.* 86, 293-300.
- 644 Bouchouicha Smida, D., Lundholm, N., Kooistra, W.H., Sahraoui, I., Ruggiero, M.V., Kotaki, Y.,
645 Ellegaard, M., Lambert, C., Hadj Mabrouk, H., Sakka Hlaili, A., 2014. Morphology and
646 molecular phylogeny of *Nitzschia bizertensis* sp. nov.—A new domoic acid-producer. *Harm.*
647 *Algae* 32, 49-63
- 648 Bruckner, C.G., Bahulikar, R., Rahalkar, M., Schink, B., Kroth, P.G., 2008. Bacteria associated
649 with benthic diatoms from Lake Constance: Phylogeny and Influences on diatom growth and
650 secretion of extracellular polymeric substances. *Appl. Environm. Microbiol.* 74, 7740–7749.
- 651 Buchan, A., LeCleir, G.R., Gulvik, C.A., González, J.M., 2014. Master recyclers: features and
652 functions of bacteria associated with phytoplankton blooms. *Nat. Rev. Microbiol.* 12, 686–
653 698.
- 654 Caporaso, J.G., Kuczynski, J., Stombaugh, J. et al., 2010. QIIME allows analysis of high-
655 throughput community sequencing data. *Nat. Methods.* 7, 335–336
- 656 Chan, S.M.N., Luan, T., Wong, M.H., Tam, N.F.Y., 2006. Removal and biodegradation of
657 polycyclic aromatic hydrocarbons by *Selenastrum capricornutum*. *Environ. Toxicol. Chem.*
658 25, 1772–1779.
- 659 Croxton, A.N., Wikfors, G.H., Schulterbrandt-Gragg, R.D., 2015. The use of flow cytometric
660 applications to measure the effects of PAHs on growth, membrane integrity, and relative
661 lipid content of the benthic diatom, *Nitzschia breviostris*. *Mar. Poll. Bull.* 91, 160–165.
- 662 Coulon, F., Chronopoulou, P.M., Fahy, A., Païssé, S., Goñi-Urriza, M., Peperzak, L., Alvarez,
663 L.A., McKew, B., Brussaard, C., Underwood, G., Timmis, K., Duran, R., McGenitya, T.,
664 2012. Central role of dynamic tidal biofilms dominated by aerobic hydrocarbonoclastic
665 bacteria and diatoms in the biodegradation of hydrocarbons in coastal mudflats. *Appl.*
666 *Environm. Microbiol.* 3638–3648.

- 667 Diaz, M., Mora, V., Pedrozo, F., Nichela, D., Baffico, G., 2015. Evaluation of native acidophilic
668 algae species as potential indicators of polycyclic aromatic hydrocarbon (PAH) soil
669 contamination. *J. Appl. Phycol.* 27, 321–325.
- 670 Dong, C., Bai, X., Sheng, H., Jiao, L., Zhou, H., Shao, Z., 2015. Distribution of PAHs and the
671 PAH-degrading bacteria in the deep-sea sediments of the high-latitude Arctic Ocean .
672 *Biogeosci.* 12, 2163–2177
- 673 Duran, R., Cravo-Laureau, C., 2016 Role of environmental factors and microorganisms in
674 determining the fate of polycyclic aromatic hydrocarbons in the marine environment. *FEMS*
675 *Microbiol. Rev.* 40, 814–830. <https://doi.org/10.1093/femsre/fuw031>.
- 676 Durán, R.E., Barra-Sanhueza, B., Salvà-Serra, F., Méndez, V., Jaén-Luchoro, D., Moore, E.R.B.,
677 Seeger, M., 2019. Complete genome sequence of the marine hydrocarbon degrader
678 *Alcaligenes aquatilis* QD168, isolated from crude oil-polluted sediment of Quintero Bay,
679 central Chile. *Microbiol. Resour. Announc.* 8, . pii: e01664-18. doi: 10.1128/MRA.01664-
680 18.
- 681 Edgar, R.C., 2010. Search and clustering orders of magnitude faster than BLAST. *Bioinformatics*
682 26, 2460–2461
- 683 Edgar, R.C., Haas, B.J., Clemente, J.C. et al., 2011. UCHIME improves sensitivity and speed of
684 chimera detection. *Bioinformatics* 27, 2194–2200
- 685 Fouilland, E., Galès, A., Beaugelin, I., Lanouguère, E., Pringault, O., Leboulanger C., 2018.
686 Influence of bacteria on the response of microalgae to contaminant mixtures. *Chemos.*, doi:
687 10.1016/j.chemosphere.2018.07.161
- 688 Foster, R.A., Kuypers, M.M., Vagner, T., Paerl, R.W., Musat, N., Zehr, J.P., 2011. Nitrogen
689 fixation and transfer in open ocean diatom-cyanobacterial symbioses. *ISME J.* 5, 1484-93.
- 690 García de Llasera, M.P., León Santiago, M., Iora Flores, E.J., Bernal Toris, D.N., Covarrubias
691 Herrera, M.R., 2017. Mini-bioreactors with immobilized microalgae for the removal
692 of benzo(a)anthracene and benzo(a)pyrene from water. *Ecol. Engine.* 121, 89-98
- 693 Ghosal, D., Ghosh, S., Dutta, T.K., Ahn, Y. 2016. Current state of knowledge in microbial
694 degradation of polycyclic aromatic hydrocarbons (PAHs): A Review. *Front. Microbiol.* Aug
695 31;7:1369. doi: 10.3389/fmicb.2016.01369.
- 696 González-Gaya, B., Martínez-Varela, A., Vila-Costa, M., Casal, P., Cerro-Gálvez, E., Berrojalbiz,
697 N., Lundin, D., Vidal, M., Mompeán, C., Bode, A., Jiménez, B., Dachs, J., 2019.
698 Biodegradation as an important sink of aromatic hydrocarbons in the oceans. *Nature*
699 *Geoscience* 12, 119–125.
- 700 Grossart H.P., Levold F., Allgaier M., Simon M., Brinkhoff T., 2005. Marine diatom species
701 harbour distinct bacterial communities. *Environ. Microbiol.* 7, 860–873. 10.1111/j.1462-
702 2920.2005.00759.x
- 703 Guillard, R.R.L., Ryther, J.H., 1962. Studies of marine planktonic diatoms. *I. *Cyclotella nana**
704 *Hustedt and *Detonula confervacea* Cleve.* *Can. J. Microbiol.* 8, 229–239.
- 705 Gutierrez, T., Green, D.H., Whitman, W.B., Nichols, P.D., Semple, K.T., Aitken, M.D., 2012.
706 *Algiphilus aromaticivorans* gen. nov., sp. nov., an aromatic hydrocarbon-degrading
707 bacterium isolated from a culture of the marine dinoflagellate *Lingulodinium polyedrum*, and
708 proposal of *Algiphilaceae* fam. nov. *Int. J. Syst. Evol. Microbiol.* 62, 2743–2749

- 709 Gutierrez, T., Singleton, D. R., Berry, D., Yang, T., Aitken, M. D., and Teske, A., 2013.
710 Hydrocarbon-degrading bacteria enriched by the Deepwater Horizon oil spill identified by
711 cultivation and DNA-SIP. *ISME J.* 7, 2091–2104. doi: 10.1038/ismej.2013.98
- 712 Haritash, A.K., Kaushik, C.P., 2009. Biodegradation aspects of polycyclic aromatic hydrocarbons
713 (PAHs): A review. *J. Hazar. Mat.* 169, 1-15.
- 714 Hong, Y.W., Yuan, D.X., Lin, Q.M., Yang, T.L., 2008. Accumulation and biodegradation of
715 phenanthrene and fluoranthene by the algae enriched from a mangrove aquatic ecosystem,
716 *Mar. Pollut. Bull.* 56, 1400–1405.
- 717 Hylland, K., 2006. Polycyclic aromatic hydrocarbon (PAH) ecotoxicology in marine ecosystems.
718 *J. Toxicol. Environ. Health A* 69, 109–123
- 719 Ibrahim, M.L., Ijah, U.J.J., Manga, S.B., Bilbis, L.S., Umar, S., 2013. Production and partial
720 characterization of biosurfactant produced by crude oil degrading bacteria. *Int. Biodeterior.*
721 *Biodegrad.* 81, 28–34
- 722 Jauffrais, T., Agoguéc, H., Gemina, M.P., Beaugeardc, M., Martin-Jézéquel, V., 2017. Effect of
723 bacteria on growth and biochemical composition of two benthic diatoms *Halamphora*
724 *coaeformis* and *Entomoneis paludosa*. *Exper. Mar. Biol. Ecol.* 495, 65–74
- 725 Jiao, N., Herndl, G.J., Hansell, D.A., Benner, R., Kattner, G., Wilhelm, S.W., Kirchman, D.L.,
726 Weinbauer, M.G., Luo, T., Chen, F., Azam, F., 2010. Microbial production of recalcitrant
727 dissolved organic matter: long-term carbon storage in the global ocean. *Nat. Rev. Microbiol.*
728 8, 593–599
- 729 Jiménez, N., Viñas, M., Guiu-Aragonés, C., Bayona, J.M., Albaigés, J., Solanas, A.M., 2011.
730 Polyphasic approach for assessing changes in an autochthonous marine bacterial community
731 in the presence of Prestige fuel oil and its biodegradation potential. *Appl. Microbiol.*
732 *Biotechnol.* 91, 823–834
- 733 Karray, F.; Ben Abdallah, M.; Kallel, N.; Hamza, M.; Fakhfakh, M.; Sayadi, S. Extracellular
734 hydrolytic enzymes produced by halophilic bacteria and archaea isolated from hypersaline
735 lake. *Mol. Biol. Rep.* 2018, 45, 1297–1309.
- 736 Kazamia, E., Czesnick, H., Van Nguyen, T.T., Croft, M.T., Sherwood, E., Sasso, S., Hodson, S.J.,
737 Warren, M.J., Smith, A.G., 2012. Mutualistic interactions between vitamin B12-dependent
738 algae and heterotrophic bacteria exhibit regulation. *Environ. Microbiol.* 14, 1466–1476.
- 739 Koedooder, C., Stock, W., Willems, A., Mangelinckx, S., De Troch, M., Vyverman, W., Sabbe,
740 K., 2019. Diatom-bacteria interactions modulate the composition and productivity of benthic
741 diatom biofilms. *Front Microbiol.* 10, 1255. doi: 10.3389/fmicb.2019.01255.
- 742 Kottuparambil, S., Agusti, S., 2018. PAHs sensitivity of picophytoplankton populations in the Red
743 Sea. *Environ. Pollut.* 239, 607-616.
- 744 Kumari, M., Ghosh, P., Thakur, I.S., 2016. Landfill leachate treatment using bacto-algal co-
745 culture: An integrated approach using chemical analyses and toxicological assessment.
746 *Ecotox. Environ. Safety.* 128, 44–51
- 747 Lafabrie, C., Sakka Hlaili, A., Leboulanger, C., Tarhouni, I., Ben Othmen, H., Mzoughi, N.,
748 Chouba, L., Pringault, O., 2013. Contaminated sediment resuspension induces shifts in the
749 structure and the functioning of phytoplankton in an eutrophic Mediterranean lagoon. *Know.*
750 *Manag. Aqua. Ecosyst.* 410, 1–16.
- 751 Lane DJ (1991) 16S/23S rRNA sequencing. In: Stackebrandt E, Goodfellow M (eds) *Nucleic*
752 *acids techniques in bacterial systematics.* Wiley, Chichester, pp 115–147

- 753 Lei, A.P., Hu, Z.L., Wong, Y.S., Tam, N.F.Y., 2007. Removal of fluoranthene and pyrene by
754 different microalgal species. *Bioresour. Technol.* 98, 273–280
- 755 L epinay, A., Turpin, T., Mondeguer, F., Grandet-Marchant, Q., Capiiaux, H., Barone, R., Lebeau.,
756 T., 2018. First insight on interactions between bacteria and the marine diatom
757 *Hasleaostrearia*: Algal growth and metabolomic fingerprinting. *Algal Res.* 31, 395–405.
- 758 Liu, Y., Luan, T. G., Lu, N.N., Lan, C.Y., 2006. Toxicity of fluoranthene and its biodegradation
759 by *Cyclotella caspia* alga. *J. Integra. Plan. Biol.* 48, 169–180.
- 760 Liu, M., Feng, J., Hu, P., Tan, L., Zhang, X., Sun, J., 2016. Spatial-temporal distributions, sources
761 of polycyclic aromatic hydrocarbons (PAHs) in surface water and suspended particular
762 matter from the upper reach of Huaihe River, China. *Ecol. Eng.* 95, 143–151
- 763 Lorenzen, C.J., Jefferey, S.W., 1980. Determination of chlorophyll in sea water. UNESCO
764 Technical Papers in Marine Science, 35. 20 p.
- 765 Lozupone, C.A., Knight, R., 2008. Species divergence and the measurement of microbial diversity.
766 *FEMS Microbiol. Revie.*, 32, 557-578
- 767 Lundholm N., Hansen, P. J., Kotaki, Y., 2004. Effect of pH on growth and domoic acid
768 production by potentially toxic diatoms of the genera *Pseudo-nitzschia* and *Nitzschia*. *Mar.*
769 *Ecol. Prog. Ser.* 273, 1-15.
- 770 Lundholm, N., Ribeiro, S., Andersen, T.J., Koch, T., Godhe, A., Ekelund, F., Ellegaard, M., 2011.
771 Buried alive –germination of up to a century-old marine protist resting stages. *Phycologia.*
772 50, 629–640
- 773 Mahdavi, H., Prasad, V., Liu, Y., Ulrich, A., 2015. In situ biodegradation of naphthenic acids in
774 oil sands tailings pond water using indigenous algae–bacteria consortium. *Bioresour.*
775 *Technol.* 187, 97–105.
- 776 McKew, B.A., Coulon, F., Osborn, A.M., Timmis, K.N., McGenity, T.J., 2007. Determining the
777 identity and roles of oil-metabolizing marine bacteria from the Thames Estuary, UK.
778 *Environ. Microbiol.* 9, 165–176.
- 779 Mei, Y., Wu, F., Wang, L., Bai, Y., Li, W., Liao, H., 2009. Binding characteristics of perylene,
780 phenanthrene and anthracene to different DOM fractions from lake water. *J. Environ. Sci.* 21,
781 414-423
- 782 Melcher, R.J., Apitz, S.E., Hemmingsen, B.B., 2002. Impact of irradiation and polycyclic aromatic
783 hydrocarbon spiking on microbial populations in marine sediment for future aging and
784 biodegradability studies. *Appl. Environ. Microbiol.* 68, 2858-2868.
- 785 Melliti Ben Garali, S., Sahraoui, I., de la Iglesia, P., Chalghaf, M., Diogene, J., Ksouri, J., Sakka
786 Hlaili, A. 2016. Effects of nitrogen supply on *Pseudo-nitzschia calliantha* and *Pseudo-nitzschia*
787 *cf. seriata*: field and laboratory experiments. *Ecotoxicol.* 25, 1211–1225.
- 788 Melliti Ben Garali, S., 2016. Diatom es toxiques au niveau des parc conchylicoles de Bizerte:
789 dynamique, diversit , toxicit  et eco-toxicologie. Thesis 322p, University of Carthage,
790 Tunisia
- 791 Mishamandani, S., Gutierrez, T., Berry, D., Aitken, M.D., 2016. Response of the bacterial
792 community associated with a cosmopolitan marine diatom to crude oil shows a preference
793 for the biodegradation of aromatic hydrocarbons. *Environ. Microbiol.* 18, 1817–1833.

- 794 Moran, M. A., Kujawinski, E. B., Stubbins, A., Fatland, R., Aluwihare, L. I., Buchan, A., Crump,
795 B. C., Dorrestein, P. C., Dyhrman, S. T., Hess, N. J., Howe, B., Longnecker, K., Medeiros,
796 P. M., Niggemann, J., Obernosterer, I., Repeta, D. J., and Waldbauer, J. R., 2016.
797 Deciphering ocean carbon in a changing world. *Proc. Natl. Acad. Sci. U.S.A.* 113, 3143–
798 3151
- 799 Moscoso, F., Teijiz, I., Deive, F. J., & Sanromán, M. A., 2012. Efficient PAHs biodegradation by
800 a bacterial consortium at flask and bioreactor scale. *Biores. Technology*, 119, 270–276.
- 801 Muñoz, R., Guieysse, B., Mattiasson, B., 2003. Phenanthrene biodegradation by an algal-bacterial
802 consortium in two-phase partitioning bioreactors. *Appl. Microbiol. Biotechnol.* 61, 261-267.
- 803 Niehus, M.C., Floeter, C., Hollert, H., Witt, G., 2018. Miniaturised marine algae test with
804 polycyclic aromatic hydrocarbons –Comparing equilibrium passive dosing and nominal
805 spiking. *Aquatic Toxicol.* 198, 190–197.
- 806 Parsons, T.P., Maita, Y., Lalli, C.M., 1984. A manual of Chemical and Biological Methods for
807 Seawater analysis. Pergamon Press, Oxford, England, vol. 1, 173.
- 808 Pikula, K. S., Zakharenko, A. M., Chaika, V. V., Stratidakis, A. K., Kokkinakis, M., Waissi, G.,
809 Golokhvast, K. S., 2019. Toxicity bioassay of waste cooking oil-based biodiesel on marine
810 microalgae. *Toxicol. Rep.* 6, 111–117
- 811 Potapova, M., Desianti, N., Enache, M., 2016. Potential effects of sediment contaminants on
812 diatom assemblages in coastal lagoons of New Jersey and New York States. *Mar. Pollut.*
813 *Bull.* 107, 453–458
- 814 Pringault, O., Lafabrie, C., Avezac, M., Bancon M.C., Carre, C., Chalhaf, M., Delpoux, S.,
815 Duvivier, A., Elbaz-Poulichet, F., Gonzalez, C., Got, P., Leboulanger, C., Spinelli, S., Sakka
816 Hlaili, A., Bouvy, M., 2016. Consequences of contaminant mixture on the dynamics and
817 functional diversity of bacterioplankton in a southwestern Mediterranean coastal
818 ecosystem. *Chemosphere.* 144, 1060-1073.
- 819 Pugazhendi, A., Abbad Wazin, H., Qari, H., Basahi, J. M. A.-B., Godon, J. J., Dhavamani, J.,
820 2016. Biodegradation of low and high molecular weight hydrocarbons in petroleum refinery
821 wastewater by a thermophilic bacterial consortium. *Environ. Technol.* 38, 2381–2391
- 822 Réveillon, D., Séchet, V., Hess, P., Amzil, Z., 2016. Production of BMAA and DAB by diatoms
823 (*Phaeodactylum tricornutum*, *Chaetoceros* sp., *Chaetocero scalcitrans* and *Thalassiosira*
824 *pseudonana*) and bacteria isolated from a diatom culture. *Harm. Algae.* 58, 45–50.
- 825 Rieck, A., Herlemann, D., Jurgens, K. and Grossart, H., 2015. Particle-associated differ from free-
826 living bacteria in surface waters of the Baltic Sea. *Front Microbiol.* 6, 1297.
- 827 San, O.N.K., Han, D., Ozkan, A.D., Angum, P., Umu, O.C.O., Tekinay, T., 2015. Journal of
828 petroleum science and engineering production and structural characterization of
829 biosurfactant produced by newly isolated *staphylococcus xylosus* STF1 from petroleum
830 contaminated soil. *J. Pet. Sci. Eng.* 133, 689–694
- 831 Seo, J.S., Keum, Y.S., Hu, Y., Lee, S.E., Li, Q.X., 2007. Degradation of phenanthrene by
832 *Burkholderia* sp. C3: initial 1, 2- and 3, 4-dioxygenation and meta- and ortho-cleavage of
833 naphthalene-1, 2-diol. *Biodeg.* 18, 123-131.
- 834 Severin, T., Bacosa, H.P., Sato, A., Erdner, D.L., 2016. Dynamics of *Heterocapsa* sp. and the
835 associated attached and free-living bacteria under the influence of dispersed and undispersed
836 crude oil. *Lett. Appl. Microbiol.* 63, 419–425. doi: 10.1111/lam.12661

- 837 Severin, T., Erdner, D.L., 2019. The phytoplankton taxon-dependent oil response and its
838 microbiome: correlation but not causation. *Frontiers in Microb.* 10, 1-14. doi:
839 10.3389/fmicb.2019.00385
- 840 Seyedsayamdost, M.R., Case, R.J., Kolter, R., Clardy, J., 2011. The Jekyll-and-Hyde chemistry of
841 *Phaeobacter gallaeciensis*. *Nat. Chem.* 3, 331–335.
- 842 Shannon, C.E., Weaver, W., 1949. The mathematical theory of communication. The University of
843 Illinois Press, Urbana, pp 1–117
- 844 Simpson, E.H., 1949. Measurement of diversity. *Nature* 163
- 845 Sison-Mangus, M.P., Jiang, S., Tran, K.N., Kudela, R.M., 2014. Host-specific adaptation governs
846 the interaction of the marine diatom, *Pseudo-nitzschia* and their microbiota. *ISME J.* 8, 63-
847 76. doi: 10.1038/ismej.2013.138.
- 848 Tang, X., He, L.Y., Tao, X.Q., Dang, Z., Guo, C.L., Lu, G.N., Yi, X.Y., 2010. Construction of an
849 artificial microalgal-bacterial consortium that efficiently degrades crude oil. *J. Hazard.*
850 *Mater.* 181, 1158-62.
- 851 Takahashi, S., Tomita, J., Nishioka, K. et al. 2014. Development of a prokaryotic universal primer
852 for simultaneous analysis of bacteria and archaea using next-generation sequencing. *PLoS*
853 *One* Aug 21;9(8):e105592. doi: 10.1371/journal.pone.0105592.
- 854 Thompson, H.F., Lesaulnier, C., Pelikanb, C., Gutierrez, T., 2018. Visualisation of the obligate
855 hydrocarbonoclastic bacteria *Polycyclovorans algicola* and *Algiphilus aromaticivorans* in
856 co-cultures with micro-algae by CARD-FISH. *Microbiol. Meth.* 152, 73–79.
- 857 Thompson, H., Angelova, A., Bowler, B., Jones, M., Gutierrez, T., 2017. Enhanced crude oil
858 biodegradation potential of natural phytoplankton-associated hydro-carbonoclastic bacteria.
859 *Environ. Microbiol.* 19, 2843–2861.
- 860 Wang, G., Tang, M., Wu, H., Dai, S., Li, T., Chen, C., He, H., Fan, J., Xiang, W., Li, X., 2016.
861 *Pyruvatibacter mobilis* gen. nov., sp. nov., a marine bacterium from the culture broth of
862 *Picochlorum* sp. 122. *Int J Syst Evol Microbiol.* 66, 184-188. doi: 10.1099/ijsem.0.000692.
- 863 Warshawsky, D., Radike, M., Jayasimhulu, K., Cody, T., 1988. Metabolism of benzo(a)pyrene by
864 dioxygenase enzyme system of the freshwater green algae *Selenastrum capricornitum*.
865 *Biochem. Biophys. Res. Comm.* 152, 540-544.
- 866 Weisburg, W.G., Barns, S.M., Pelletier, D.A., Lane, D.J. 1991. 16S ribosomal DNA amplification
867 for phylogenetic study. *J. Bacteriol.* 173, 697–703
- 868 Wilcke, W., 2007. Global patterns of polycyclic aromatic hydrocarbons (PAHs) in soil. *Geoderma.*
869 141, 157–166.
- 870 Yang, C., Liu, Y., Zhu, Y., Zhang, Y., 2016. Insights into the binding interactions of autochthonous
871 dissolved organic matter released from *Microcystis aeruginosa* with pyrene using
872 spectroscopy. *Mar. Pollut. Bull.* 104, 113-120
- 873 Yirui, W., Tengeng, H., Mingqi, Z., Yueling, Z., Enmin, L., Tongwang, H., Zhong, H., 2009.
874 Isolation of marine benzo[a]pyrene-degrading *Ochrobactrum* sp. BAP5 and proteins
875 characterization. *J. Environ. Sci.* 21, 1446–1451
- 876 Yuan, J., Lai, Q., Sun, F., Zheng, T., Shao, Z., 2015. The diversity of PAH-degrading bacteria in
877 a deep-sea water column above the Southwest Indian Ridge. *Front Microbiol.* 6, 853. doi:
878 10.3389/fmicb.2015.00853

879 [Zhuang, W.Q., Tay, J.H., Maszenan, A.M., Krumholz, L.R., Tay, S.T.](#) 2003. Importance of Gram-
880 positive naphthalene-degrading bacteria in oil-contaminated tropical marine sediments. [Lett.](#)
881 [Appl. Microbiol.](#) 36(4), 251-7.
882

883

884

885

886

887

888

889

890

891

892

893

894

895

896

897

898

899

900

901

902

903

904

905

906 **Table 1**
 907 Exponential growth rate (d^{-1}) of *Nitzschia sp.* grown under non-axenic and axenic conditions in
 908 control (C) and contaminated treatments by two PAHs (BaP and Flt). Values are means \pm
 909 standard deviations, letters indicate homogenous group, r^2 is coefficient of determination
 910

Treatment	Non-axenic	Axenic
C	0.50 ± 0.01^c ($r^2 = 0.94$)	0.43 ± 0.03^b ($r^2 = 0.85$)
BaP	0.44 ± 0.009^b ($r^2 = 0.96$)	0.35 ± 0.002^a ($r^2 = 0.90$)
Flt	0.45 ± 0.0003^b ($r^2 = 0.93$)	0.41 ± 0.016^b ($r^2 = 0.91$)

911
 912
 913 **Table 2**
 914 Theoretical and measured concentrations of Flt and BaP in *Nitzschia sp.* cultures under
 915 different conditions (axenic, non-axenic and sterile)
 916 Values are means \pm standard deviations
 917

Measured concentrations	Theoretical concentration	
	Flt ($256 \mu\text{g L}^{-1}$)	BaP ($3 \mu\text{g L}^{-1}$)
Axenic	238.11 ± 4.68	2.53 ± 0.42
Non-axenic	250.79 ± 2.65	2.36 ± 0.27
Sterile, light	255.68 ± 3.09	2.59 ± 0.43
Sterile, dark	242.39 ± 4.10	2.65 ± 0.41

918
 919
 920
 921
 922
 923
 924
 925
 926
 927

928
 929
 930
 931
 932
 933
 934
 935
 936

Table 3

The % of PAHs (BaP and Flt) accumulated in cells (%PAH_{acc}), remaining in the medium (%PAH_{dis}) and degraded by all processes (%PAH_{deg}), including abiotic process [photo-oxidation (%PAH_{pho}), volatilization (%PAH_{vol}) and adsorption (%PAH_{ads})] and biodegradation by microorganisms (%PAH_{biodeg}) [by diatom (%PAH_{diadeg}) or by bacteria (%PAH_{bacdeg})], in the *Nitzschia sp.* culture under non axenic and axenic conditions. Values are mean ± standard deviation.

	BaP		Flt	
	non-axenic	axenic	non-axenic	axenic
%PAH_{acc}	18.1 ± 1.6	52.8 ± 3.0	11.3 ± 1.5	33.0 ± 2.0
%PAH_{dis}	2.5 ± 0.6	8.5 ± 1.4	0.5 ± 0.0	5.6 ± 1.3
%PAH_{deg}	79.4 ± 2.3	38.7 ± 2.0	88.2 ± 4.2	61.4 ± 4.1
%PAH _{pho}	10.0 ± 1.8	10.0 ± 1.8	7.9 ± 1.1	7.9 ± 1.1
%PAH _{vol}	0	0	0	0
%PAH _{ads}				
%PAH _{biodeg}	69.4 ± 2.6	28.7 ± 2.6	80.3 ± 5.2	53.5 ± 3.2
%PAH _{diadeg}	28.7 ± 2.6	28.7 ± 2.6	53.5 ± 3.2	53.5 ± 3.2
%PAH _{bacdeg}	2.6		3.2	
%PAH _{bacdeg}	40.7 ± 2.5		26.8 ± 2.2	

937
 938
 939
 940
 941
 942
 943
 944
 945
 946
 947
 948

Figure captions

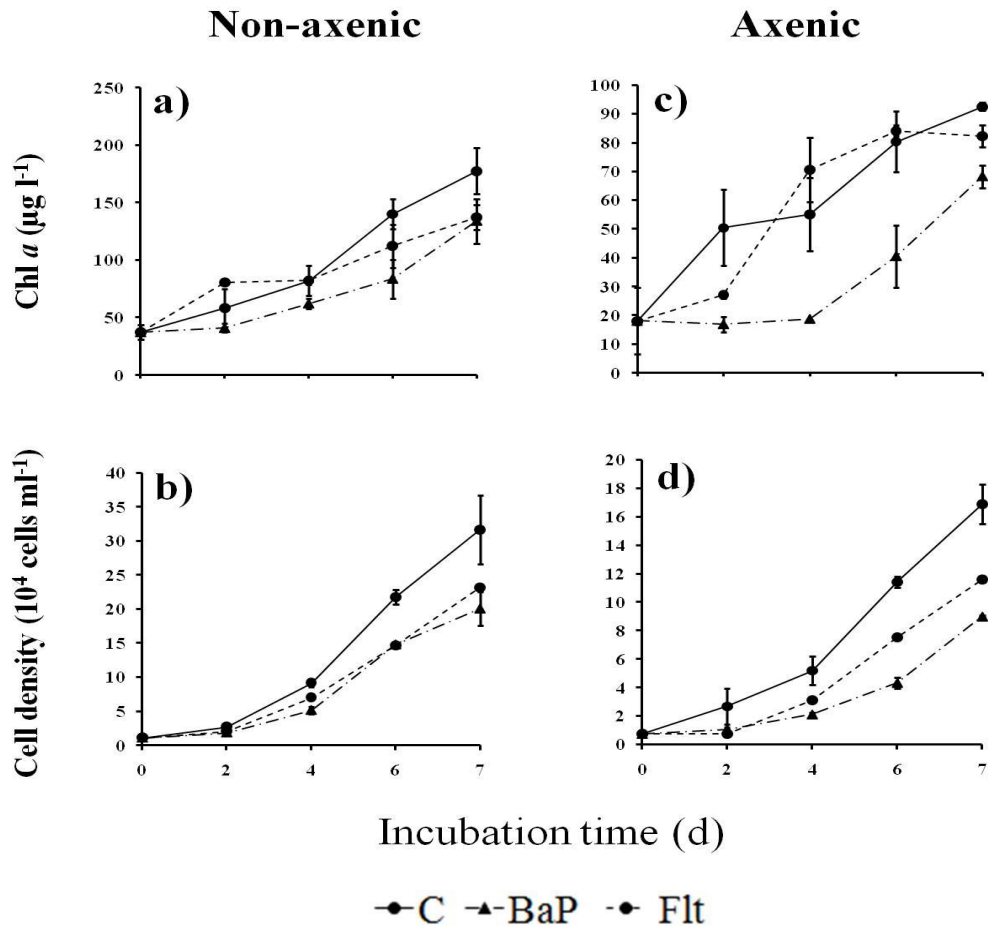
949
950
951
952
953
954
955
956
957
958
959
960
961
962
963
964
965
966

967
968
969
970
971
972
973
974
975
976
977

Fig. 1. Temporal evolution of Chl *a* concentration and growth kinetics of *Nitzschia sp.* under non-axenic (a and b) and axenic (c and d) conditions in control (C) and contaminated treatments by BaP and Ft. Values are means \pm standard deviations.

Fig. 2. Relative abundance of microbial communities in attached (AB) and free-living bacteria (FB) from *Nitzschia sp.* Culture. **A.** Relative phylogenetic abundance was based on frequencies of 16S rRNA gene sequences affiliated with archaea and bacterial phyla or proteobacterial classes in AB and FB fractions. **B.** Major genera from dominant OTU (>1% of all sequences) in AB and FB fractions. **C.** Venn diagram showing the distribution of prokaryotic measurable OTUs in AB and FB samples.

Fig. 3. Phylogenetic tree based on similarities of 16S rRNA sequences of bacterial isolates and its relatives. The tree was based on the Juke-Cantor model and the Neighbor-Joining method with bootstrap values for 1000 replicates. The *scale bar* represents 5% estimated sequence divergence. The archaeal sequence of *Natrinema altunense* was used as the outgroup



992

993

Fig. 1

994

995

996

997

998

999

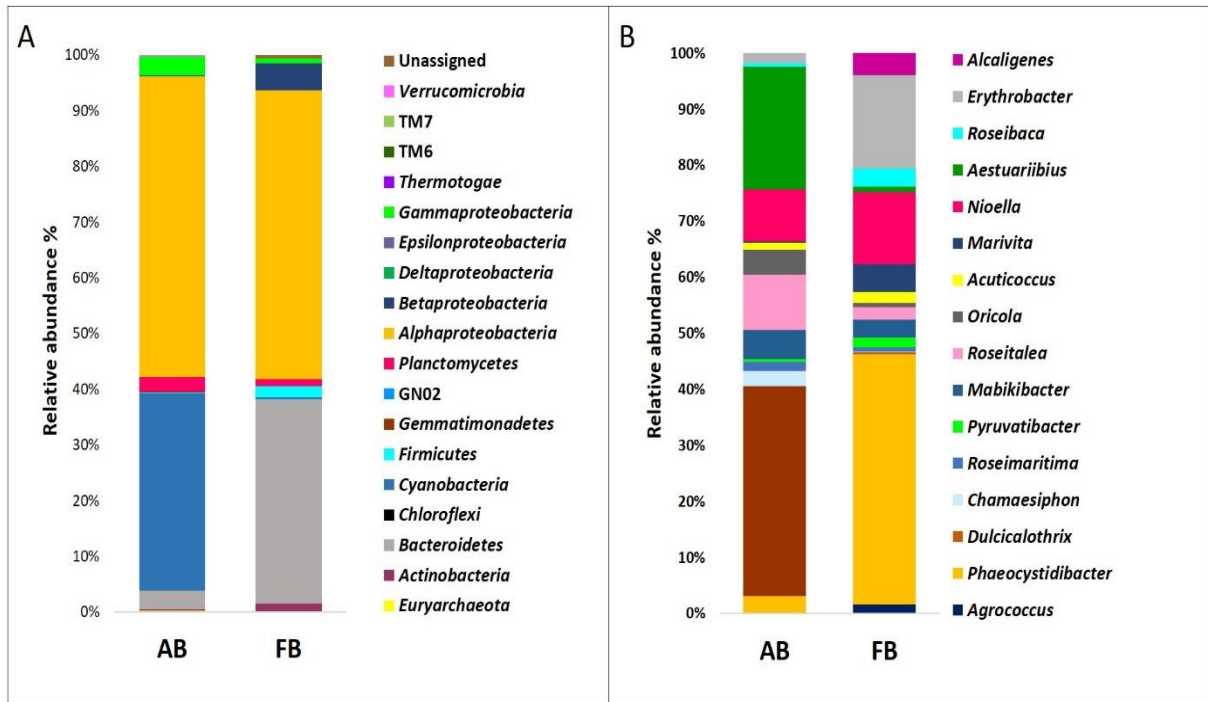
1000

1001

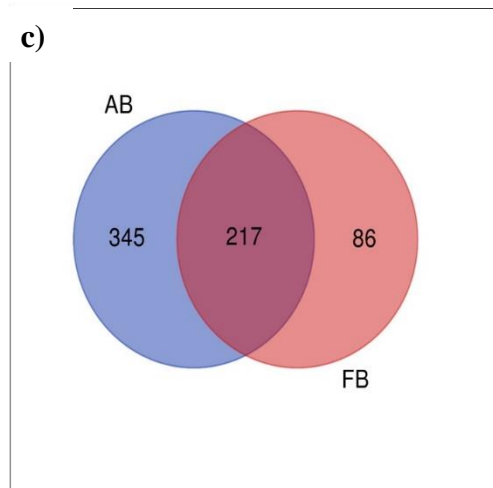
1002

a)

b)



1003



1004

1005

1006

1007

1008

1009

1010

1011

1012

1013

Fig. 2

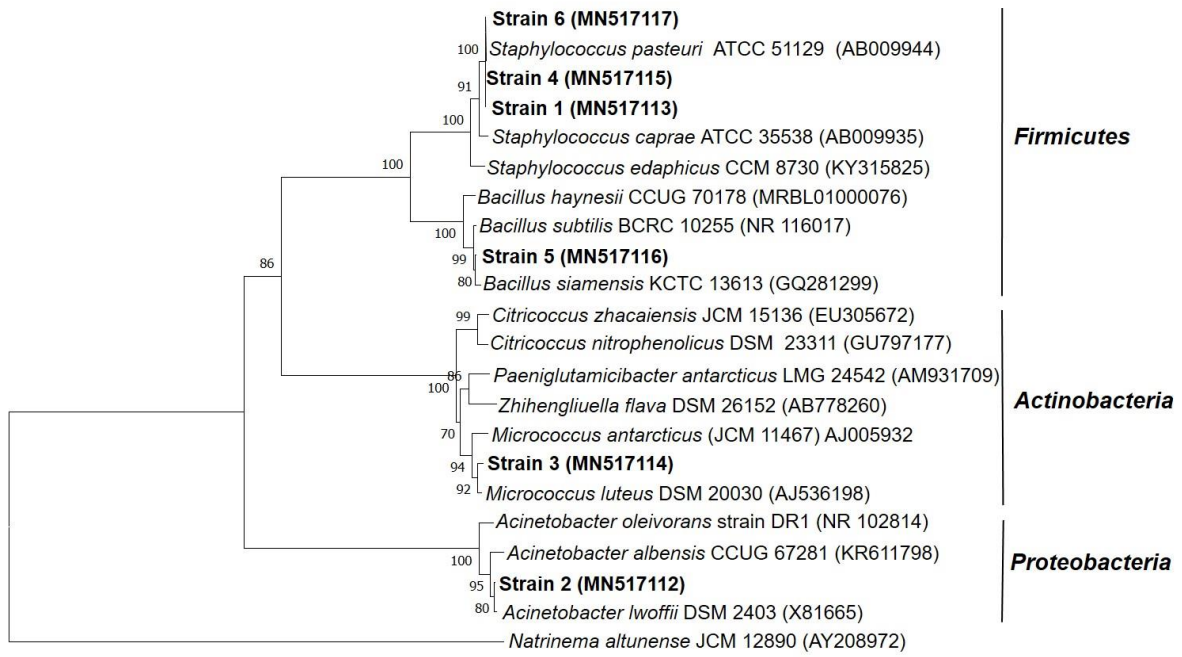


Fig. 3

1014

1015

1016

1017

1018

1019

1020

1021

1022

1023

1024

1025

1026

1027

1028

1029

1030

1031